Pharmaceutical Research, Vol. 23, No. 6, June (© 2006)
DOI: 10.1007/s11095-006-0067-2

Research Paper

ATP-Binding Cassette Transporter G2 Mediates the Efflux of Phototoxins on the Luminal Membrane of Retinal Capillary Endothelial Cells

Tomoko Asashima,[1,2,3] Satoko Hori,[1,2,3] Sumio Ohtsuki,[1,2,3] Masanori Tachikawa,[1] Masahiko Watanabe,[4] Chisato Mukai,[5] Shinji Kitagaki,[5] Naoki Miyakoshi,[5] and Tetsuya Terasaki[1,2,3,6]

Received October 3, 2005; accepted January 25, 2006

Purpose. The purpose of this study was to clarify the localization and function of the ATP-binding cassette transporter G2 (ABCG2; BCRP/MXR/ABCP) in retinal capillary endothelial cells, which form the inner blood–retinal barrier, as an efflux transport system.
Methods. The expression was determined by reverse transcriptase polymerase chain reaction and Western blotting. The localization was identified by immunostaining. The transport function of ABCG2 was measured by flow cytometry.
Results. Western blotting indicated that ABCG2 was expressed as a glycosylated disulfide-linked complex in the mouse retina and in peripheral tissues, including liver, kidney, and small intestine. Double immunolabeling of ABCG2 and glucose transporter 1 suggested that ABCG2 was localized on the luminal membrane of mouse retinal capillary endothelial cells. ABCG2 mRNA and protein were found to be expressed in a conditionally immortalized rat retinal capillary endothelial cell line, TR-iBRB, and rat retina. Treatment with Ko143, an ABCG2 inhibitor, restored the accumulation of pheophorbide a and protoporphyrin IX in TR-iBRB cells.
Conclusion. ABCG2 is expressed on the luminal membrane of retinal capillary endothelial cells, where ABCG2 acts as the efflux transporter for photosensitive toxins such as pheophorbide a and protoporphyrin IX. ABCG2 could play an important role at the inner blood–retinal barrier in restricting the distribution of phototoxins and xenobiotics in retinal tissue.

KEY WORDS: ABC half-transporter; ABCG2/BCRP/MXR/ABCP; inner blood–retinal barrier; pheophorbide a; retinal capillary endothelial cell.

INTRODUCTION

The blood–retinal barrier (BRB) is composed of two layers, an inner layer of retinal capillary endothelial cells and an outer layer of retinal pigmented epithelial (RPE) cells, which regulate the exchange of various compounds, including nutrients, drugs, and toxins, between the blood and the retina using various transporter molecules (1). Understanding the transport mechanisms at the inner BRB will provide important information about the effective delivery of drugs to the retina, but so far, only a very limited number of transporters have been identified here, such as glucose transporter 1 (GLUT1), monocarboxylate transporter 1, organic anion transporting polypeptides 2, and P-glycoprotein (P-gp).

The ATP-binding cassette transporter G2 (ABCG2; BCRP, MXR, or ABCP) is known to act as an efflux transporter not only in cancer cells (2) but also in normal tissues such as the liver, small intestine, and mammary gland (3–6). It has also been reported to play an important role in the absorption, distribution, and elimination of drugs that are ABCG2 substrates, including dietary carcinogens and anticancer agents. However, no study has reported the expression of functional ABCG2 at the inner BRB.

ABCG2 transports light-sensitive compounds including pheophorbide a (PhA), a chlorophyll-derived dietary phototoxin related to porphyrin, and another phototoxin, protoporphyrin IX (PPIX) (3). The retina is a highly photosensitive organ that is vulnerable to light-induced damage caused by a variety of phototoxic compounds, including porphyrins (7). Indeed, RPE cells have been shown to be damaged by treatment with PPIX (8). The elimination mechanism for transporting phototoxins out of the retina is as yet unknown, and the nature of the substrate specificity at the inner BRB

[1] Department of Molecular Biopharmacy and Genetics, Graduate School of Pharmaceutical Sciences, Tohoku University, Aoba, Aramaki, Aoba-ku, Sendai 980-8578, Japan.
[2] New Industry Creation Hatchery Center, Tohoku University, Aoba, Aramaki, Aoba-ku, Sendai 980-8579, Japan.
[3] CREST and SORST of Japan Science and Technology Agency (JST), Japan.
[4] Department of Anatomy, Hokkaido University School of Medicine, Sapporo 060-8638, Japan.
[5] Division of Pharmaceutical Sciences, Graduate School of Natural Science and Technology, Kanazawa University, Kakuma-machi, Kanazawa 920-1192, Japan.
[6] To whom correspondence should be addressed. (e-mail: terasaki@mail.pharm.tohoku.ac.jp)

ABBREVIATIONS: ABC, ATP-binding cassette; GLUT1, glucose transporter 1; P-gp, P-glycoprotein; PhA, pheophorbide a; PPIX, protoporphyrin IX.

raises the possibility that ABCG2 may act as an elimination system of phototoxins in the retina. Clarifying the localization and function of ABCG2 will also provide us with important information about drug distribution into the retina.

The purpose of this study was to investigate the localization and function of ABCG2 at the inner BRB to clarify the involvement of ABCG2 in the efflux transport system at the inner BRB, using PhA, PPIX, and a conditionally immortalized cell line.

MATERIALS AND METHODS

Animals

C57 BL/6J male mice (6 weeks) were purchased from Charles River (Yokohama, Japan). ABCG2 knockout mice were obtained from Deltagen (San Carlos, CA, USA). All experiments were carried out according to the requirements of the Animal Care Committee, Graduate School of Pharmaceutical Sciences, Tohoku University.

Reagents

Pheophorbide a was purchased from Frontier Scientific Inc. (Logan, UT, USA), and *N*-glycosidase F (NGF) was obtained from Roche Applied Science (Penzberg, Germany). All other chemicals were commercial products of analytic grade.

Synthesis of Ko143

Ko143 was synthesized according to the procedure developed by Nakagawa *et al.* (9,10). L-Tryptophan was converted into *cis*-1-isobutyl-7-methoxy-3-methoxycarbonyl-1, 2,3,4-tetrahydro-β-carboline, known as compound A, which was then condensed with Z-Glu(OBu^t)-OH (11) in the presence of dicyclohexylcarbodiimide to form the corresponding amide. Treatment with 10% Pd-C and ammonium formate resulted in debenzyloxycarbonylation and spontaneous ring closure to produce Ko143 ($[\alpha]_D^{26}$ −101.4 (*c* 0.3, MeOH), lit. (12) $[\alpha]_D^{26}$ −99.8 (*c* 0.6, MeOH)). Further information concerning the transformation of compound A into Ko143 is available from the authors.

Cell Culture

TR-iBRB2 cells were established from rat retinal endothelial cells and characterized as described previously (13). HEK293/rABCG2myc cells, which overexpress rat ABCG2, were established as described previously (14).

Western Blot Analysis

Crude cell membranes were prepared and Western blot analysis was carried out as reported previously (14–16). Antipeptide polyclonal antibodies were raised in guinea pigs against amino acid residues 1–34 (G2-Ab1) and 305–343 (G2-Ab2) of mouse ABCG2 (GenBank accession number AF140218), as reported previously (14). G2-Ab1 (1 μg/mL) was used for rat tissues and TR-iBRB cells, whereas G2-Ab2 (0.5 μg/mL) was used for mouse tissues. Horseradish peroxidase (HRP)-conjugated goat anti-guinea pig IgG was purchased from ICN Pharmaceuticals Inc. (Aurora, OH, USA).

Immunohistochemical Analysis

Adult mice anesthetized with ketamine and xylazine were perfused with 4% formaldehyde in phosphate-buffered saline (PBS). Paraffin sections 5 μm thick were cut from the kidney, small intestine, and eyeball and were pretreated with 10 μg/mL pepsin (DAKO, Glostrup, Denmark) in 0.2 N HCl at 37°C for 7 min. For the labeling of mouse ABCG2 alone, sections were incubated at 20°C for 1 h, 5 μg/mL fluorescein isothiocyanate (FITC)-conjugated goat anti-guinea pig IgG was used as a secondary antibody, and then the nuclei were stained with 6.6 μM propidium iodide. For double-immunofluorescence staining, sections were incubated overnight with 1 μg/mL guinea pig anti-mouse ABCG2 antibody, 10 μg/mL mouse anti-Na^+–K^+-ATPase α-1 (Upstate Biotech, Lake Placid, NY, USA), and/or rabbit anti-GLUT1 antibody (1:5000; Chemicon, Temecula, CA, USA) at 20°C, or with normal IgG, as a negative control. The sections were then incubated at 20°C for 2 h with FITC- or rhodamine-labeled secondary antibodies as follows: FITC-conjugated goat anti-guinea pig IgG (5 μg/mL; ICN Pharmaceuticals Inc.), rhodamine-conjugated goat anti-mouse IgG (5 μg/mL; Beckman Coulter Inc., Fullerton, CA, USA), or rhodamine-conjugated swine anti-rabbit IgG (6.5 μg/mL; DAKO). The sections were viewed by confocal laser microscopy (TCS SP; Leica Microsystems Heidelberg GmbH, Mannheim, Germany), and the images obtained were reconstructed using Leica confocal software (LCS; Leica). In the retina, immunoreactivity was detected by means of the streptavidin–biotin immunoperoxidase method using biotinylated goat anti-guinea pig IgG (1:200; DAKO) and HRP-conjugated streptavidin (Nichirei, Tokyo, Japan) as the secondary antibody. Digital images were obtained with an Axio Cam and were reconstructed using AxioVision software (Carl Zeiss, Thornwood, NY, USA).

Reverse Transcriptase Polymerase Chain Reaction

Total cellular RNA was prepared from PBS-washed cells using RNeasy Mini Kits (QIAGEN, Tokyo, Japan) according to the manufacturer's instructions. Complementary DNA (cDNA) was synthesized from 1 μg total RNA using oligo $(dT)_{15}$ as a primer and Moloney murine leukemia virus (M-MLV) reverse transcriptase (ReverTraAce, Toyobo Co. Ltd., Osaka, Japan). Reverse transcriptase polymerase chain reaction (RT-PCR) was carried out using Takara Ex Taq™ (Takara Shuzo Co. Ltd., Shiga, Japan) according to the manufacturer's instructions. The sequences of sense and antisense primers were as follows: sense primer, 5′-CAATGGGATCATGAAACCTG-3′ and antisense primer, 5′-GAGGCTGATGAATGGAGAA-3′ for ABCG2 (GenBank accession number AB105817); sense primer, 5′-TTTGAGACCTTCAACACCCC-3′ and antisense primer, 5′-ATAGCTCTTCTCCAGGGAGG-3′ for β-actin (GenBank accession number NM_031144). The PCR was carried out by using an initial melting procedure at 85°C for 3 min, adding the primers (hot start method), and amplification for

34 cycles (ABCG2) or 25 cycles (β-actin) via denaturation for 1 min at 94°C, annealing for 1 min at 60°C with an extension of 1 min at 72°C, followed by a final extension at 72°C for 10 min. The PCR products were separated on 2% agarose gel and stained with ethidium bromide.

Transport Assay

HEK293 or HEK293/rABCG2myc cells, at a density of 3×10^5 cells/tube, were incubated for 30 min at 37°C in extracellular fluid (ECF) buffer [122 mM NaCl, 25 mM $NaHCO_3$, 3 mM KCl, 1.4 mM $CaCl_2$, 2 mM $MgSO_4$, 0.4 mM K_2HPO_4, 10 mM D-glucose, 10 mM HEPES (pH 7.4), 290 ± 15 mOsm/kg, under O_2 ventilation] with or without 2 μM Ko143, a rat ABCG2-specific inhibitor (12,14). After a 30-min preincubation period, the cells were washed with ECF buffer, resuspended in 10 nM PhA in ECF buffer, with or without 2 μM Ko143, and incubated for a further 1 h at 37°C. The uptake time after 60 min was selected to demonstrate efflux transporter function because the uptake of PhA has reached steady state. The cells were then washed with ice-cold ECF buffer and placed on ice until use. PhA was determined by flow cytometry using a 635-nm red diode laser and a 661-nm band-pass filter (FACS Calibur; BD Biosciences, San Jose, CA, USA). The flow cytometry parameters such as voltage and amp gain were optimized in each experiment. A minimum of 10,000 cells were collected for each sample, and debris was eliminated by gating on forward *vs.* side scatter. Analyses were performed using CellQuest™ software (BD Biosciences). The geometric mean value in each FL4 fluorescence histogram was used as PhA fluorescence data. TR-iBRB2 cells were seeded at a density of 4×10^4 cells/well in rat-tail collagen-I-coated 24-well plates (BD Bioscience, Bedford, MA, USA) and cultured for 72 h at 33°C. Transport studies were performed at 37°C. After removing the culture medium and washing with ECF buffer, the cells were pretreated at 37°C for 30 min in the presence or absence of 2 μM Ko143. Uptake was initiated by adding 10 nM PhA in ECF buffer, with or without 2 μM Ko143, and continued for 1 h at 37°C. The efflux transporter activity was terminated by replacing the solution with ice-cold ECF buffer. The cells were trypsinized at 4°C and placed on ice until required for measurement. Flow cytometry was performed as described above. For the transport assay of PPIX, uptake was initiated by adding 10 nM PPIX in ECF buffer, with or without 5 μM Ko143. PPIX was determined by flow cytometry using a 488-nm argon laser and a 650-nm band-pass filter (FACS Calibur). The geometric mean value in each FL3 fluorescence histogram was used as PPIX fluorescence data.

The experiments were performed at least in triplicate and produced similar results. Cell viability was assessed by the Trypan blue extrusion method (Trypan blue concentration, 0.25%), and the proportion of viable cells was between 98 and 100% under all experimental conditions examined.

Data Analysis

Unless otherwise indicated, all data represent the mean ± SEM. An unpaired, two-tailed Student's *t* test was used to determine the significance of differences between two group means. One-way analysis of variance (ANOVA) followed by the modified Fisher's least-squares difference method was used to assess the statistical significance of differences among means of more than two groups.

RESULTS

Expression of ABCG2 and Complex Formation in the Mouse Retina

Western blot analysis of crude membrane fractions from adult mouse retina, kidney, liver, and small intestine was performed (Fig. 1). In the retina, a single band at about 75 kDa with anti-ABCG2 antibody, under reducing conditions, was detected with a long exposure, but no band was detected after a short exposure. A single band with the same size was also detected in all other tissues. Following treatment with NGF, the size of the band was significantly reduced to about 60 kDa. In the absence of 2-mercaptoethanol (2-ME), a band of approximately 170 kDa was seen in all tissues including the retina.

Localization of ABCG2 in the Mouse Retina and Other Tissues

To determine the location of ABCG2 protein in the mouse retina, sections from wild-type mice (+/+) and ABCG2 knockout mice (−/−) were labeled immunohistochemically with antibodies against ABCG2 (Fig. 2). In the retina of wild-type mice, immunoreactivity was detected in retinal capillary endothelial cells, using the streptavidin–biotin immunoperoxidase method (black arrowheads; Fig. 2A). In knockout mice (−/−; Fig. 2B), no signal was observed, indicating that the immunoreactivity shown in Fig. 2A was specifically confined to ABCG2 in the mouse retina. Immunoreactivity of ABCG2 in RPE cells was detected in wild-type mice, and similar reactivity in RPE cells was also detected in knockout mice using the streptavidin–biotin immunoperoxidase method (data not shown). For detailed analysis, double labeling for ABCG2 (Fig. 2C and E, green) and GLUT1 (Fig. 2D and E, red) was per-

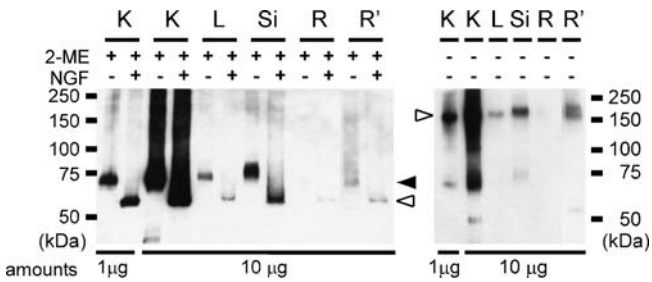

Fig. 1. Western blot analysis of ABCG2 in mouse retina and peripheral tissues. Crude membrane proteins were prepared from kidney (K), liver (L), small intestine (Si), and retina (R and R′ for 10 s and 10 min exposure, respectively). Membrane proteins were untreated [NGF(−)] or treated with NGF [NGF(+)] and denatured in the presence [2-ME(+)] or absence [2-ME(−)] of 2-mercaptoethanol. Sodium dodecyl sulfate polyacrylamide gel electrophoresis (7.5%) was used to separate 1- or 10-μg aliquots per lane.

formed. GLUT1 has been reported to be expressed on both the luminal and abluminal membranes in retinal capillaries (17,18). Labeled ABCG2 was detected inside the GLUT1 signal (Fig. 2E), suggesting a luminal location of ABCG2 in retinal capillary endothelial cells.

In sections of kidney from wild-type mice (+/+), ABCG2 labeling was detected on the luminal membranes of renal tubules, and the signal did not overlap with staining for the Na^+–K^+-ATPase α-1 subunit, a marker for the basolateral membrane of distal tubules (19) (Fig. 2F). In the small intestine, ABCG2 was localized on the brush border of the epithelial cells in the villi (Fig. 2H). The mucus-secreting goblet cells, which are scattered in the intestinal epithelium, were negative for ABCG2 (white arrowhead; Fig. 2H). No labeling was detected in any of the tissues from knockout mice (−/−; Fig. 2G and I).

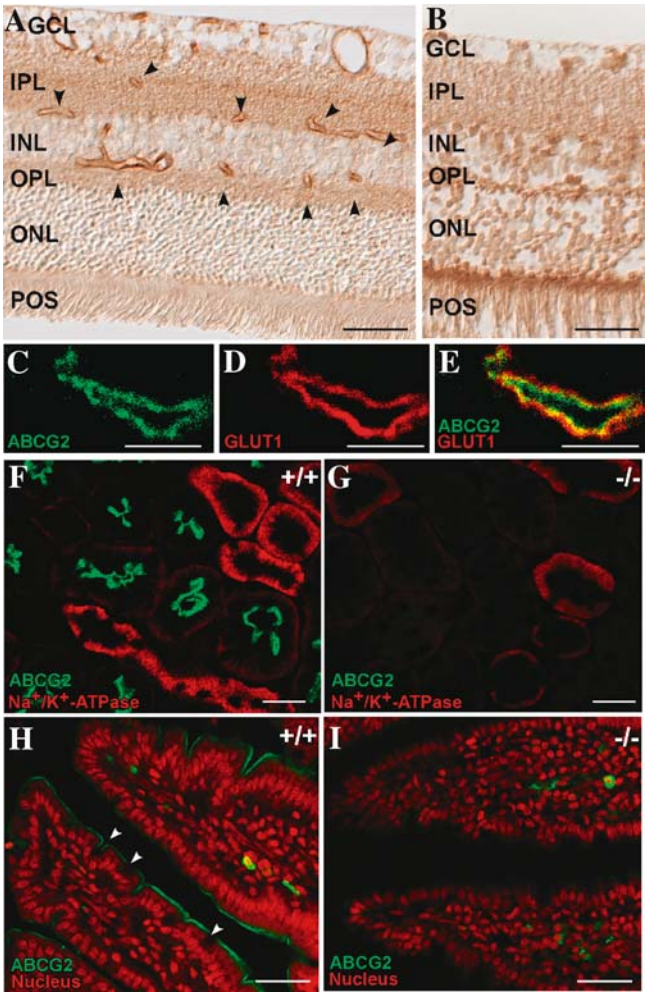

Fig. 2. Localization of ABCG2 protein in mouse retina, kidney, and small intestine. (A and B) Immunolabeling of ABCG2 in the retina of wild-type (A) and knockout (B) mice using the streptavidin–biotin immunoperoxidase method. GCL, Ganglion cell layer; IPL, inner plexiform layer; INL, inner nuclear layer; OPL, outer plexiform layer; ONL, outer nuclear layer; POS, photoreceptor outer segments. Scale bars, 40 μm. (C–E) Immunolabeling of ABCG2 (C; green) and GLUT1 (D; red) in retinal capillaries of wild-type mice. E is the merged image of C and D. Scale bars, 5 μm. (F and G) Immunolabeling of ABCG2 (green) and Na^+–K^+-ATPase α-1 subunit (red) in kidney from wild-type (F) and knockout (G) mice. Scale bars, 20 μm. (H and I) Immunolabeling of ABCG2 (green) and propidium iodide (red, nuclei) in the small intestine of wild-type (H) and knockout (I) mice. White arrowheads indicate goblet cells. Scale bars, 40 μm.

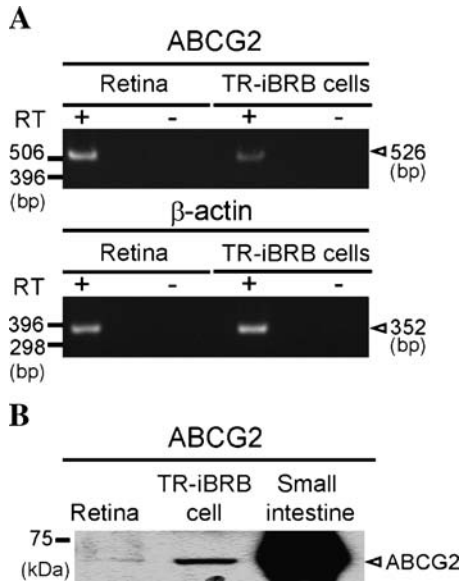

Fig. 3. Expression of ABCG2 mRNA and protein in rat retina and the conditionally immortalized rat retinal capillary endothelial cell line, TR-iBRB. (A) One microgram of total RNA was reverse transcribed, and 0.1 μg cDNA was amplified by polymerase chain reaction. RNA samples that were not reverse transcribed [RT(−)] were used as negative controls for DNA contamination. (B) Western blot analysis. Crude membrane proteins were prepared from retina, TR-iBRB cells, and small intestine. Membrane proteins were denatured in the presence of 2-mercaptoethanol. Sodium dodecyl sulfate polyacrylamide gel electrophoresis (7.5%) was used to separate 50 μg aliquots per lane.

Rat ABCG2 mRNA and Protein Expression in TR-iBRB2 Cells

Reverse transcriptase polymerase chain reaction analysis was performed to determine the mRNA expression of

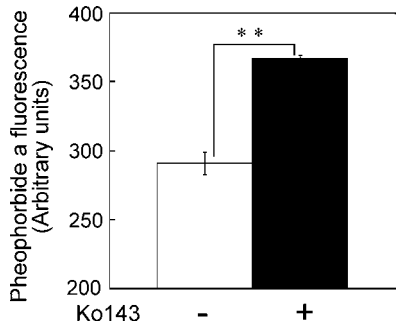

Fig. 4. Accumulation of PhA in TR-iBRB cells. PhA accumulation in TR-iBRB cells exposed to 10 nM PhA for 1 h at 37°C in the presence (filled column) or absence (open column) of 2 μM Ko143. PhA fluorescence is in arbitrary units, determined by flow cytometry with a 635-nm laser and a 661-nm band-pass filter. Each column represents the mean fluorescence ± SEM (n = 5–6). $^{**}p < 0.01$, significant difference.

ABCG2 in TR-iBRB2 cells, which are conditionally immortalized rat retinal capillary endothelial cells (Fig. 3A). Bands of the expected size for rat ABCG2 (526 bp) and β-actin (352 bp) were obtained in both retina and TR-iBRB2 cells. The nucleotide sequence of the product was identical to that of rat ABCG2 (GenBank accession number AB105817). In the Western blot analysis of the rat retina, TR-iBRB cells, and small intestine, a band at about 75 kDa was detected with anti-ABCG2 antibody, under reducing conditions (Fig. 3B).

Cellular Efflux of PhA Mediated by ABCG2 in TR-iBRB2 Cells

The transport function of ABCG2 on retinal capillary endothelial cells was evaluated by measuring the accumulation of PhA in TR-iBRB2 cells. The accumulation of PhA in TR-iBRB2 cells after 60 min was significantly increased by treatment with 2 μM Ko143, a specific inhibitor of human, rat, and mouse ABCG2 (12,14) (Fig. 4). The transport of PhA by rat ABCG2 and the inhibitory effect of Ko143 were further investigated using HEK293 cells. In HEK293/rABCG2myc cells, which overexpress ABCG2, the accumulation of PhA was significantly reduced compared with parental HEK293 cells (Fig. 5), and treatment with Ko143 restored PhA accumulation to the level seen in parental HEK293 cells in the absence of Ko143. In contrast, Ko143 had no effect on the accumulation of PhA in parental HEK293 cells.

Cellular Efflux of PPIX Mediated by ABCG2 in TR-iBRB2 Cells

The transport function of ABCG2 on retinal capillary endothelial cells was evaluated by measuring the accumulation of PPIX in TR-iBRB2 cells. The accumulation of PPIX in TR-iBRB2 cells after 60 min was significantly increased by treatment with 5 μM Ko143 (Fig. 6).

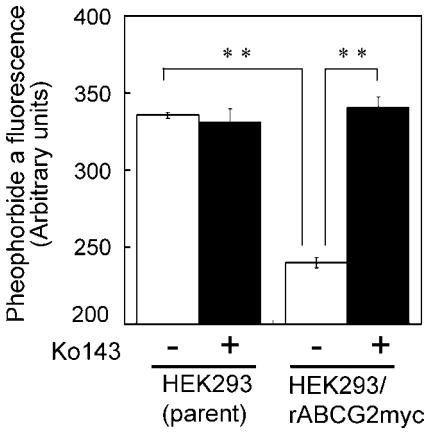

Fig. 5. Efflux of PhA from cells overexpressing rat ABCG2. HEK293 cells and HEK293/rABCG2myc cells were exposed to 10 nM PhA for 1 h at 37°C with (filled column) or without (open column) 2 μM Ko143. PhA fluorescence is in arbitrary units, determined by flow cytometry with a 635-nm laser and a 661-nm band-pass filter. Each column represents the mean fluorescence ± SEM (n = 3–5). $^{**}p < 0.01$, significant difference.

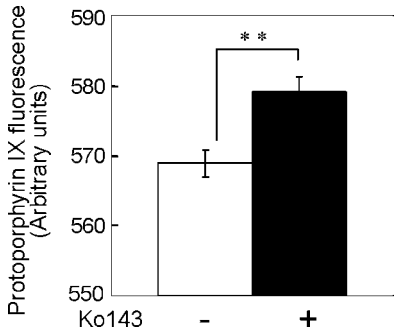

Fig. 6. Accumulation of PPIX in TR-iBRB cells. PPIX accumulation in TR-iBRB cells exposed to 10 nM PPIX for 1 h at 37°C in the presence (filled column) or absence (open column) of 5 μM Ko143. PPIX fluorescence is in arbitrary units, determined by flow cytometry with a 488-nm laser and a 650-nm band-pass filter. Each column represents the mean fluorescence ± SEM (n = 5–6). $^{**}p < 0.01$, significant difference.

DISCUSSION

In this study, we have demonstrated the involvement of ABCG2 in PhA transport as well as its expression and localization at the inner BRB. In the retina, as well as the kidney, small intestine, and liver, ABCG2 was expressed as an N-glycosylated protein (Fig. 1), which was very similar in size to that reported for mouse ABCG2 protein in brain capillaries (16). The transport function of exogenous human ABCG2 has been reported to be inhibited in dominant-negative mutants, suggesting that ABCG2 forms homodimers to function as an efflux transporter (20). As shown in Fig. 1, in the absence of 2-ME, ABCG2 migrated as a band of approximately 170 kDa, consistent in size with a dimer, in the mouse retina and other peripheral tissues. This result indicates that ABCG2 forms a disulfide-bonded complex in the mouse retina.

Immunohistochemical analysis showed that ABCG2 was expressed in capillary endothelial cells in the retina (Fig. 2) but not in other retinal cells such as glial cells and neurons. Retinal capillary endothelial cells are polarized, with luminal and abluminal surfaces, controlling the direction of transport across the BRB. The results of the double-immunolabeling experiments suggested that ABCG2 was localized to the luminal membrane of retinal capillary endothelial cells and would, therefore, mediate transport from inside endothelial cells to the blood. The immunoreactivity in RPE cells was similar in wild-type and knockout mice using the streptavidin–biotin immunoperoxidase method, but the expression of ABCG2 in RPE cells cannot be confirmed in the present immunohistochemical study. This is likely due to the fact that the antibody reacted with protein(s) other than ABCG2 protein in RPE cells. As shown in the right panel of Fig. 1, a weak band at around 50 kDa was detected in the retina and kidney under 2-ME-free conditions, suggesting that it is possible that anti-ABCG2 antibody reacts with proteins other than the ABCG2 protein in these tissues. For this reason, in this study, the immunoreactivities of the anti-ABCG2 antibody were compared between wild-type and knockout mice to determine the localization of ABCG2 proteins.

In the mouse kidney and small intestine, the results showed that ABCG2 was localized to the luminal membranes of proximal renal tubules and the apical membranes of epithelial cells in small intestinal villi. This result confirms a previous report that was conducted using single immunostaining (3).

TR-iBRB2 cells are conditionally immortalized rat retinal capillary endothelial cells, which can be used as an *in vitro* model of the inner BRB for transport and regulation studies, although it is unclear whether the cells retain their polarity (21). Since TR-iBRB cells have been established from rats, the following functional study was conducted using rat ABCG2. TR-iBRB2 cells expressed ABCG2 mRNA and protein (Fig. 3), and the accumulation of PhA in these cells was significantly increased by treatment with the ABCG2 inhibitor, 2 μM Ko143 (Fig. 4). Although PhA is transported by human and mouse ABCG2 (3,22), variants of human ABCG2, such as R482, have been reported to exhibit altered substrate specificity (23). As far as R482 is concerned, the amino acid corresponding to R482 in the isolated rat ABCG2 is also arginine (14), and human ABCG2 variants of R482T and R482G have been reported to transport PhA (22). The accumulation of PhA in cells overexpressing rat ABCG2 was lower than that in parental cells (Fig. 5), showing that PhA is a substrate of the rat ABCG2 transporter. Retinal capillary endothelial cells are also known to express P-gp (21). However, a previous report using a cell line overexpressing P-gp, Multidrug resistance protein-1 (MRP1), or ABCG2 suggested that PhA is a selective substrate for ABCG2 among these transporters (22). Furthermore, Ko143, which inhibits P-gp and MRP1 at least 200 times less effectively than ABCG2 (12), inhibited the excretion of PhA from cells overexpressing ABCG2 (Fig. 5). Therefore, ABCG2 functions as an efflux transporter in TR-iBRB2 cells and excretes PhA from these cells.

For it to accumulate in the cells, PhA has to be able to enter the cells. To our knowledge, there is no report that PhA is a substrate of other types of transporters, e.g., organic anion transporters (OATs), organic anion transporting polypeptides (OATPs), organic cation transporters (OCTs), and monocarboxylate transporters (MCTs). Since PhA has been reported to be a lipophilic compound (24,25), it is possible that PhA enters the TR-iBRB cells by passive diffusion.

In view of the results presented here, we suggest that ABCG2 functions on the luminal side of the inner BRB to excrete substrates, including PhA, into the blood. As substrates of ABCG2 include natural products, such as porphyrins, endogenous substrates (including sulfated conjugates of sterols), and xenobiotics (including anticancer drugs) (26,27), it is likely that ABCG2 has a role in excluding all these compounds from the retina. Endogenous porphyrin, PPIX, is a substrate of ABCG2 because ABCG2-expressing cells accumulate less PPIX (3,28) in various organs of the body (29,30). The accumulation of PPIX in TR-iBRB cells was increased by treatment with the ABCG2 inhibitor, 5 μM Ko143 (Fig. 6), suggesting that PPIX was excreted by ABCG2 from retinal endothelial cells. Since PPIX is a phototoxic intermediate of the heme metabolic pathway, ABCG2 would play an important role in preventing the accumulation of phototoxic intermediates in the retina by acting as a detoxification system. Dehydroepiandrosterone sulfate is an endogenous substrate of ABCG2 (31) and has been detected in the rat retina (32–34). Therefore, ABCG2 may also be involved in maintaining neuroactive steroid levels in the retina. To clarify the physiological function of ABCG2 in the retina, further studies regarding substrate accumulation in the retina and retinal morphology of ABCG2 knockout mice are necessary.

Imatinib mesylate (STI571), which is an inhibitor of platelet-derived growth factor, c-kit, and v-abl receptor kinases, has been reported to be transported *in vitro* and *in vivo* by ABCG2, which limits its distribution into the brain (35,36). Imatinib mesylate is successfully used in the treatment of gastrointestinal stromal tumors, based on its inhibition of c-kit receptor tyrosine kinase (KIT) activity. The observation that almost 20% of retinoblastomas are KIT positive suggests that these tumors are good candidates for imatinib mesylate therapy (37). This study suggests that ABCG2 at the inner BRB could affect the retinal distributions of drugs, including imatinib mesylate. Furthermore, recent studies have identified many single nucleotide polymorphisms in the ABCG2 gene (38,39), which alter the transporter function of ABCG2 (40–43). Such polymorphisms may change the retinal distribution of ABCG2 substrates, and people who either lack ABCG2 activity or have only low levels may have an increased susceptibility to retinal photosensitivity.

CONCLUSION

In conclusion, this study has demonstrated that ABCG2 is localized to the luminal membrane of mouse retinal capillary endothelial cell where it exists as a glycosylated, disulfide-linked complex and acts as an efflux transporter to reduce the cellular accumulation of PhA and PPIX, phototoxic compounds. Strategies for drug delivery to the retina should consider that P-gp, as well as ABCG2, acts as an efflux transporter at the inner BRB.

ACKNOWLEDGMENTS

We would like to thank Mr. N. Kimura for technical assistance and Ms. N. Funayama for secretarial assistance. We would like to thank Drs. Ken-ichi Hosoya and Masatoshi Tomi of University of Toyama for valuable suggestions. This work was supported in part by a Grant-in-Aid for Scientific Research from the Ministry of Education, Culture, Sports, Science and Technology (MEXT) and Japan Society for the Promotion of Science (JSPS) and a 21st Century Center of Excellence (COE) Program from JSPS. It was also supported in part by the Industrial Technology Research Grant Program from the New Energy and Industrial Technology Development Organization (NEDO) of Japan.

REFERENCES

1. P. A. Stewart and U. I. Tuor. Blood–eye barriers in the rat: correlation of ultrastructure with function. *J. Comp. Neurol.* **340**:566–576 (1994).

2. Y. Liu, H. Peng, and J. T. Zhang. Expression profiling of ABC transporters in a drug-resistant breast cancer cell line using AmpArray. *Mol. Pharmacol.* **68**:430–438 (2005).
3. J. W. Jonker, M. Buitelaar, E. Wagenaar, M. A. van der Valk, G. L. Scheffer, R. J. Scheper, T. Plosch, F. Kuipers, R. P. Elferink, H. Rosing, J. H. Beijnen, and A. H. Schinkel. The breast cancer resistance protein protects against a major chlorophyll-derived dietary phototoxin and protoporphyria. *Proc. Natl. Acad. Sci. USA* **99**:15649–15654 (2002).
4. A. E. van Herwaarden, J. W. Jonker, E. Wagenaar, R. F. Brinkhuis, J. H. Schellens, J. H. Beijnen, and A. H. Schinkel. The breast cancer resistance protein (Bcrp1/Abcg2) restricts exposure to the dietary carcinogen 2-amino-1-methyl-6-phenylimidazo[4,5-b]pyridine. *Cancer Res.* **63**:6447–6452 (2003).
5. J. W. Jonker, G. Merino, S. Musters, A. E. van Herwaarden, E. Bolscher, E. Wagenaar, E. Mesman, T. C. Dale, and A. H. Schinkel. The breast cancer resistance protein BCRP (ABCG2) concentrates drugs and carcinogenic xenotoxins into milk. *Nat. Med.* **11**:127–129 (2005).
6. G. Merino, A. E. van Herwaarden, E. Wagenaar, J. W. Jonker, and A. H. Schinkel. Sex-dependent expression and activity of the ATP-binding cassette transporter breast cancer resistance protein (BCRP/ABCG2) in liver. *Mol. Pharmacol.* **67**:1765–1771 (2005).
7. M. Boulton, M. Rozanowska, and B. Rozanowski. Retinal photodamage. *J. Photochem. Photobiol. B.* **64**:144–161 (2001).
8. L. A. Bynoe, L. V. Del Priore, and R. Hornbeck. Photosensitization of retinal pigment epithelium by protoporphyrin IX. *Graefe Arch. Clin. Exp. Ophthalmol.* **236**:230–233 (1998).
9. M. Taniguchi, T. Anjiki, M. Nakagawa, and T. Hino. Formation and reactions of the cyclic tautomers of tryptophans and tryptamines. VII. Hydroxylation of tryptophans and tryptamines. *Chem. Pharm. Bull.* **32**:2544–2554 (1984).
10. M. Nakagawa, H. Fukushima, T. Kawate, M. Hongou, T. Une, S. Kodato, M. Taniguchi, and T. Hino. Synthetic approaches to fumitremorgins. III. Synthesis of optically active pentacyclic ring systems, and their oxidation at ring C. *Chem. Pharm. Bull.* **37**:23–32 (1989).
11. P. Chevallet, P. Garrouste, B. Malawska, and J. Martinez. Facile synthesis of tert-butyl ester of N-protected amino acids with tert-butyl bromide. *Tetrahedron Lett.* **34**:7409–7412 (1993).
12. J. D. Allen, A. van Loevezijn, J. M. Lakhai, M. van der Valk, O. van Tellingen, G. Reid, J. H. Schellens, G. J. Koomen, and A. H. Schinkel. Potent and specific inhibition of the breast cancer resistance protein multidrug transporter in *vitro* and in mouse intestine by a novel analogue of fumitremorgin C. *Mol. Cancer Ther.* **1**:417–425 (2002).
13. K. Hosoya, M. Tomi, S. Ohtsuki, H. Takanaga, M. Ueda, N. Yanai, M. Obinata, and T. Terasaki. Conditionally immortalized retinal capillary endothelial cell lines (TR-iBRB) expressing differentiated endothelial cell functions derived from a transgenic rat. *Exp. Eye Res.* **72**:163–172 (2001).
14. S. Hori, S. Ohtsuki, M. Tachikawa, N. Kimura, T. Kondo, M. Watanabe, E. Nakashima, and T. Terasaki. Functional expression of rat ABCG2 on the luminal side of brain capillaries and its enhancement by astrocyte-derived soluble factor(s). *J. Neurochem.* **90**:526–536 (2004).
15. S. Hori, S. Ohtsuki, M. Ichinowatari, T. Yokota, T. Kanda, and T. Terasaki. Selective gene silencing of rat ATP-binding cassette G2 transporter in an in *vitro* blood–brain barrier model by short interfering RNA. *J. Neurochem.* **93**:63–71 (2005).
16. M. Tachikawa, M. Watanabe, S. Hori, M. Fukaya, S. Ohtsuki, T. Asashima, and T. Terasaki. Distinct spatio-temporal expression of ABCA and ABCG transporters in the developing and adult mouse brain. *J. Neurochem.* **95**:294–304 (2005).
17. K. Takata, T. Kasahara, M. Kasahara, O. Ezaki, and H. Hirano. Ultracytochemical localization of the erythrocyte/HepG2-type glucose transporter (GLUT1) in cells of the blood–retinal barrier in the rat. *Invest. Ophthalmol. Vis. Sci.* **33**:377–383 (1992).
18. A. K. Kumagai, S. A. Vinores, and W. M. Pardridge. Pathological upregulation of inner blood–retinal barrier Glut1 glucose transporter expression in diabetes mellitus. *Brain Res.* **706**:313–317 (1996).
19. E. Arystarkhova, R. K. Wetzel, and K. J. Sweadner. Distribution and oligomeric association of splice forms of Na(+)–K(+)-ATPase regulatory gamma-subunit in rat kidney. *Am. J. Physiol. Renal. Physiol.* **282**:393–407 (2002).
20. K. Kage, S. Tsukahara, T. Sugiyama, S. Asada, E. Ishikawa, T. Tsuruo, and Y. Sugimoto. Dominant-negative inhibition of breast cancer resistance protein as drug efflux pump through the inhibition of S–S dependent homodimerization. *Int. J. Cancer* **97**:626–630 (2002).
21. K. Hosoya and M. Tomi. Advances in the cell biology of transport via the inner blood–retinal barrier: establishment of cell lines and transport functions. *Biol. Pharm. Bull.* **28**:1–8 (2005).
22. R. W. Robey, K. Steadman, O. Polgar, K. Morisaki, M. Blayney, P. Mistry, and S. E. Bates. Pheophorbide a is a specific probe for ABCG2 function and inhibition. *Cancer Res.* **64**:1242–1246 (2004).
23. E. M. Smigielski, K. Sirotkin, M. Ward, and S. T. Sherry. dbSNP: a database of single nucleotide polymorphisms. *Nucleic Acids Res.* **28**:352–355 (2000).
24. P. Grellier, R. Santus, E. Mouray, V. Agmon, J. C. Maziere, D. Rigomier, A. Dagan, S. Gatt, and J. Schrevel. Photosensitized inactivation of Plasmodium falciparum- and Babesia divergens-infected erythrocytes in whole blood by lipophilic pheophorbide derivatives. *Vox Sang.* **72**:211–220 (1997).
25. B. Pegaz, E. Debefve, F. Borle, J. P. Ballini, H. van den Bergh, and Y. N. Kouakou-Konan. Encapsulation of porphyrins and chlorins in biodegradable nanoparticles: the effect of dye lipophilicity on the extravasation and the photothrombic activity. A comparative study. *J. Photochem. Photobiol. B.* **80**:19–27 (2005).
26. J. D. Allen and A. H. Schinkel. Multidrug resistance and pharmacological protection mediated by the breast cancer resistance protein (BCRP/ABCG2). *Mol. Cancer Ther.* **1**:427–434 (2002).
27. B. L. Abbott. ABCG2 (BCRP) expression in normal and malignant hematopoietic cells. *Hematol. Oncol.* **21**:115–130 (2003).
28. P. Krishnamurthy and J. D. Schuetz. The ABC transporter Abcg2/ Bcrp: role in hypoxia mediated survival. *BioMetals* **18**:349–358 (2005).
29. P. Venkatesh, S. P. Garg, E. Kumaran, and H. K. Tewari. Congenital porphyria with necrotizing scleritis in a 9-year-old child. *Clin. Experiment. Ophthalmol.* **28**:314–318 (2000).
30. S. Thunell, P. Harper, and A. Brun. Porphyrins, porphyrin metabolism and porphyrias. IV. Pathophysiology of erythropoietic protoporphyria—diagnosis, care and monitoring of the patient. *Scand. J. Clin. Lab. Invest.* **60**:581–604 (2000).
31. M. Suzuki, H. Suzuki, Y. Sugimoto, and Y. Sugiyama. ABCG2 transports sulfated conjugates of steroids and xenobiotics. *J. Biol. Chem.* **278**:22644–22649 (2003).
32. A. Lanthier and V. V. Patwardhan. *In vitro* steroid metabolism by rat retina. *Brain Res.* **463**:403–406 (1988).
33. P. Guarneri, R. Guarneri, C. Cascio, P. Pavasant, F. Piccoli, and V. Papadopoulos. Neurosteroidogenesis in rat retinas. *J. Neurochem.* **63**:86–96 (1994).
34. C. Cascio, R. Guarneri, D. Russo, G. De Leo, M. Guarneri, F. Piccoli, and P. Guarneri. Pregnenolone sulfate, a naturally occurring excitotoxin involved in delayed retinal cell death. *J. Neurochem.* **74**:2380–2391 (2000).
35. H. Burger, H. van Tol, A. W. Boersma, M. Brok, E. A. Wiemer, G. Stoter, and K. Nooter. Imatinib mesylate (STI571) is a substrate for the breast cancer resistance protein (BCRP)/ABCG2 drug pump. *Blood* **104**:2940–2942 (2004).
36. P. Breedveld, D. Pluim, G. Cipriani, P. Wielinga, O. Tellingenvan, A. H. Schinkel, and J. H. Schellens. The effect of Bcrp1 (Abcg2) on the *in vivo* pharmacokinetics and brain penetration of imatinib mesylate (Gleevec): implications for the use of breast cancer resistance protein and P-glycoprotein inhibitors to enable the brain penetration of imatinib in patients. *Cancer Res.* **65**:2577–2582 (2005).
37. D. Bosch, M. Pache, R. Simon, P. Schraml, K. Glatz, M. Mirlacher, J. Flammer, G. Sauter, and P. Meyer. Expression and amplification of therapeutic target genes in retinoblastoma. *Graefe Arch. Clin. Exp. Ophthalmol.* **243**:156–162 (2005).
38. A. Iida, S. Saito, A. Sekine, C. Mishima, Y. Kitamura, K. Kondo, S. Harigae, S. Osawa, and Y. Nakamura. Catalog of 605 single-nucleotide polymorphisms (SNPs) among 13 genes encoding human ATP-binding cassette transporters: ABCA4, ABCA7, ABCA8, ABCD1, ABCD3, ABCD4, ABCE1, ABCF1, ABCG1,

ABCG2, ABCG4, ABCG5, and ABCG8. *J. Hum. Genet.* **47**: 285–310 (2002).
39. T. Ishikawa, H. Endou, K. Inui, A. Tsuji, M. Wada, and Y. Sumino. The pharmacogenomics of drug transporters: functional analysis approaches. *Tanpakushitsu Kakusan Koso* **49** (12): 2024–2034 (2004).
40. Y. Imai, M. Nakane, K. Kage, S. Tsukahara, E. Ishikawa, T. Tsuruo, Y. Miki, and Y. Sugimoto. C421A polymorphism in the human breast cancer resistance protein gene is associated with low expression of Q141K protein and low-level drug resistance. *Mol. Cancer Ther.* **1**:611–616 (2002).
41. Y. Honjo, K. Morisaki, L. M. Huff, R. W. Robey, J. Hung, M. Dean, and S. E. Bates. Single-nucleotide polymorphism (SNP) analysis in the ABC half-transporter ABCG2 (MXR/BCRP/ABCP1). *Cancer Biol. Ther.* **1**:696–702 (2002).
42. H. Mitomo, R. Kato, A. Ito, S. Kasamatsu, Y. Ikegami, I. Kii, A. Kudo, E. Kobatake, Y. Sumino, and T. Ishikawa. A functional study on polymorphism of the ATP-binding cassette transporter ABCG2: critical role of arginine-482 in methotrexate transport. *Biochem. J.* **373**:767–774 (2003).
43. S. Mizuarai, N. Aozasa, and H. Kotani. Single nucleotide polymorphisms result in impaired membrane localization and reduced atpase activity in multidrug transporter ABCG2. *Int. J. Cancer* **109**:238–246 (2004).